

Tuning the Topology Structures of Polymolybdate-based Hybrids from Interpenetrated Framework to Interdigitated Architecture *via* Changing Polymolybdate Clusters†

Shaobin Li, Li Zhang, Huiyuan Ma*, Haijun Pang* and Chunyan Zhao

Key Laboratory of Green Chemical Engineering and Technology of College of Heilongjiang Province, College of Chemical and Environmental Engineering, Harbin University of Science and Technology, Harbin 150040, China Tel.: 86-0451-86392716, Fax: 86-0451-86392716; E-mail: mahy017@163.com (Ma H. Y.), panghj116@163.com (Pang. H. J.).

Table of contents:

1. **Table S1** All of the H-bonds in **3**.
2. **Fig. S1**. View of the detailed formation process of the 2D layer in **3**.
3. **Fig. S2** The IR spectra of compounds **1-3**.
4. **Fig. S3** Output of a calculated powder X-ray pattern by POWDER CELL for compounds **1-3**.
5. **Fig. S4** The plots of the anodic and the cathodic peak currents for wave I of **1-** (a), **2-** (b) and **3-**CPE (c) against scan rates, respectively.
6. **Fig. S5** Reduction of IO_3^- for **1-** (a), **2-** (b) and **3-**CPEs (c) in 1M H_2SO_4 solution.
7. **Fig. S6** The linear dependence of the cathodic catalytic current of wave I for **1-** (a), **2-** (b) and **3-**CPE (c), with IO_3^- concentration, respectively.
8. **Fig. S7** The 40 consecutive CV cycles of the **1**, **2** and **3**-CPEs at the scan rate of $50 \text{ mV}\cdot\text{s}^{-1}$.

Table S1 All of the H-bonds in **3**.

| D-H...A ^a | D-H | H...A | D...A | ∠D-H...A |
|----------------------|------|-------|-------|----------|
| C8-H8...O8 | 0.93 | 2.487 | 3.407 | 169.81 |
| C8-H8...O16 | 0.93 | 2.549 | 3.066 | 115.50 |
| C15-H15...O5 | 0.93 | 2.597 | 3.302 | 132.98 |
| C13-H13...O13 | 0.93 | 2.242 | 3.112 | 155.50 |
| C3-H3...O7 | 0.93 | 2.515 | 3.275 | 138.99 |
| C9-H9...O2 | 0.93 | 2.426 | 3.257 | 148.80 |
| C5-H5...O14 | 0.93 | 2.648 | 3.462 | 146.59 |
| C6-H6...O15 | 0.93 | 2.658 | 3.343 | 131.01 |
| C17-H17...O14 | 0.93 | 2.476 | 3.404 | 176.45 |
| C24-H24...O18 | 0.93 | 2.494 | 3.412 | 169.03 |

^aD = donor atom, A = acceptor atom.

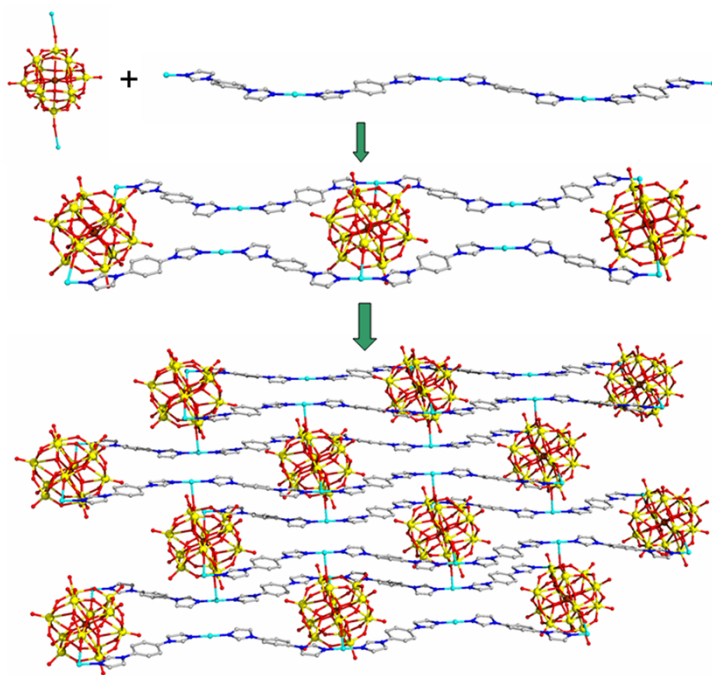


Fig. S1. View of the detailed formation process of the 2D layer in **3**.

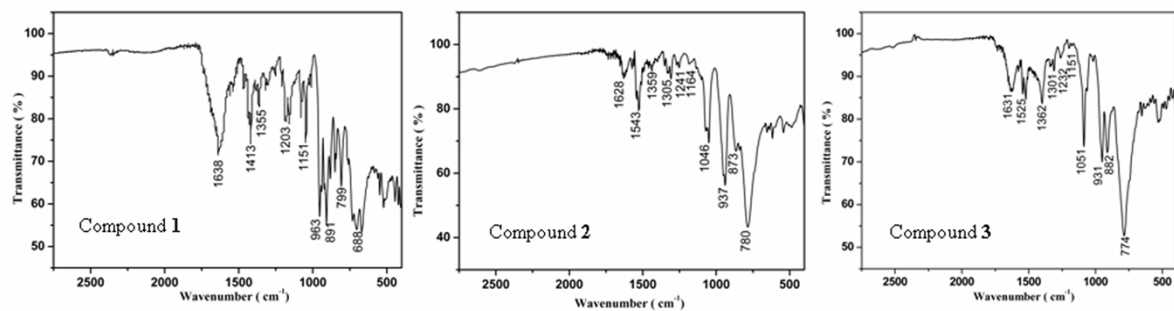


Fig. S2. The IR spectra of copounds **1-3**.

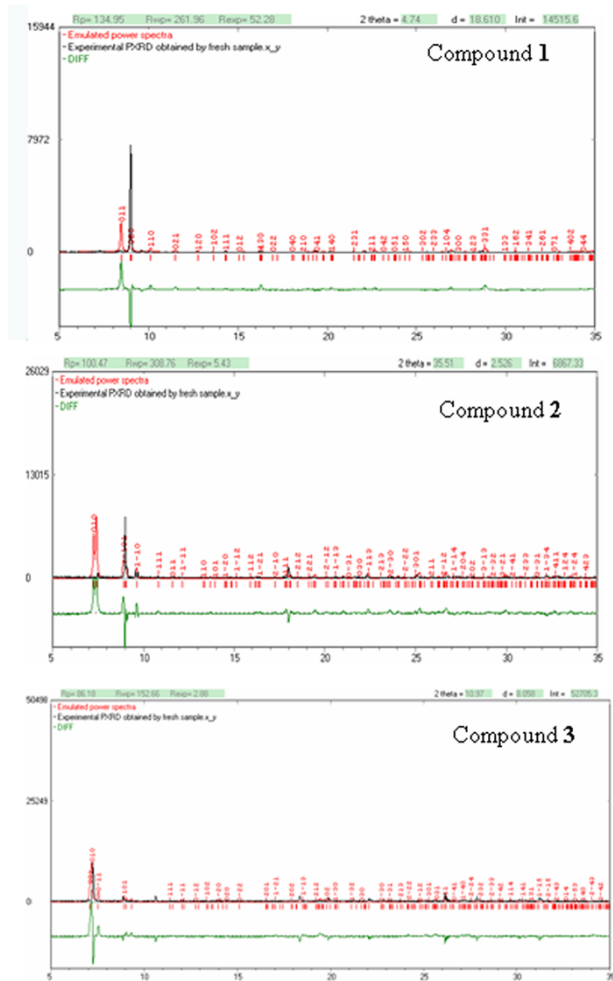


Fig. S3. Output of a calculated powder X-ray pattern by POWDER CELL for compounds 1-3.

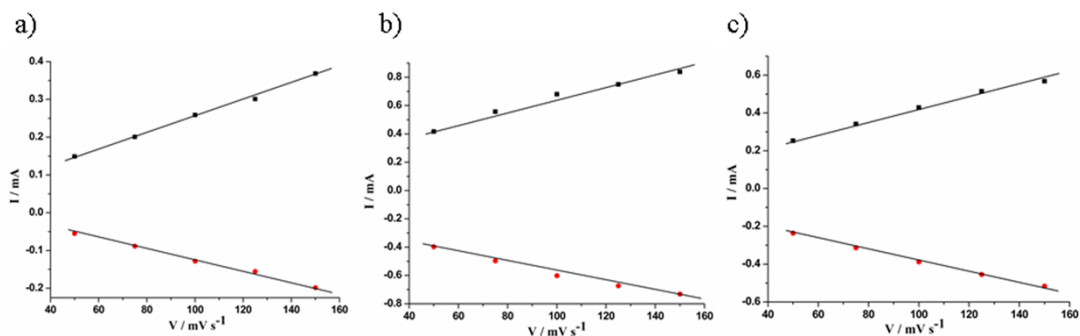


Fig. S4. The plots of the anodic and the cathodic peak currents for wave I of 1- (a), 2- (b) and 3-CPE (c) against scan rates, respectively.

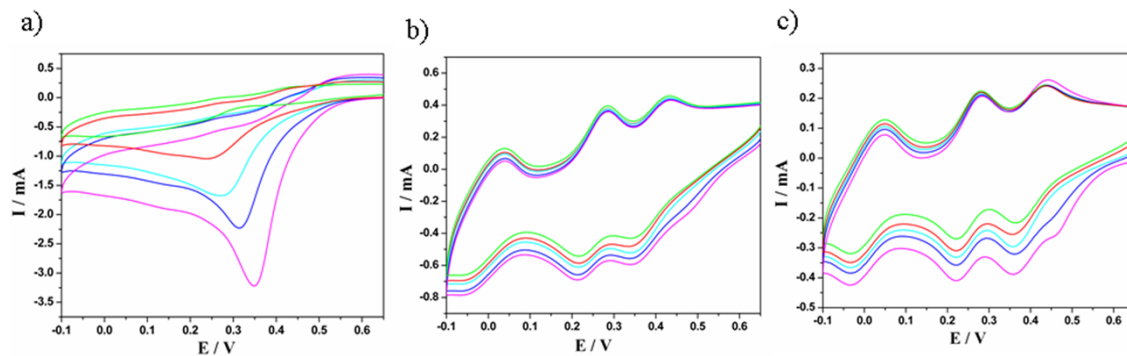


Fig. S5. Reduction of IO_3^- for **1-** (a), **2-** (b) and **3-CPEs** (c) in 1M H_2SO_4 solution (scan rate: $50 \text{ mV}\cdot\text{s}^{-1}$). The concentrations (from inner to outer) are 0, 5, 10, 15, 20 mM for IO_3^- respectively.

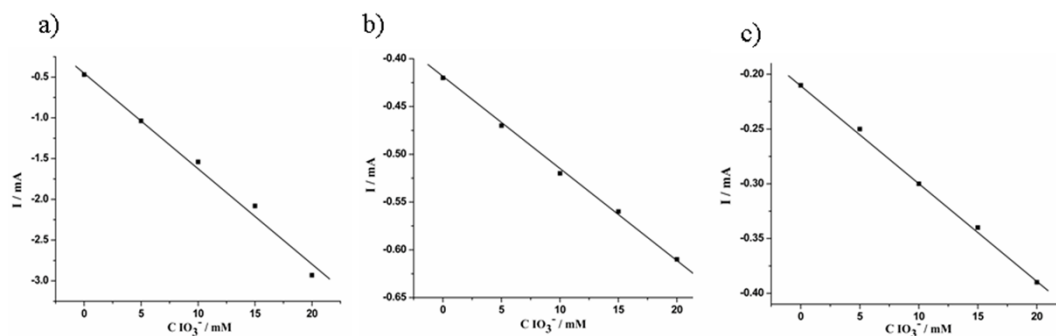


Fig. S6. The linear dependence of the cathodic catalytic current of wave I for **1-** (a), **2-** (b) and **3-CPE** (c), with IO_3^- concentration, respectively.

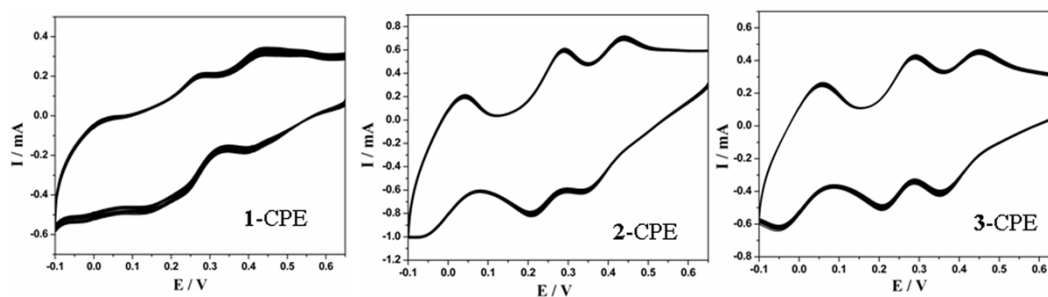


Fig. S7. The 40 consecutive CV cycles of the **1-**, **2-** and **3-CPEs** at the scan rate of $50 \text{ mV}\cdot\text{s}^{-1}$.